

Investigation of mean volume fraction fluctuations on the mean drag force acting on spherical particle assemblies

by

Jacob Vogts

A thesis submitted to the graduate faculty

in partial fulfillment of the requirements for the degree of

MASTER OF SCIENCE

Major: Mechanical Engineering

Program of Study Committee:
Alberto Passalacqua, Major Professor
Rodney O. Fox
Shankar Subramaniam

The student author, whose presentation of the scholarship herein was approved by the program of study committee, is solely responsible for the content of this thesis. The Graduate College will ensure this thesis is globally accessible and will not permit alterations after a degree is conferred.

Iowa State University

Ames, Iowa

2018

Copyright © Jacob Vogts, 2018. All rights reserved.

TABLE OF CONTENTS

LIST OF FIGURES	iii
LIST OF TABLES	iv
NOMENCLATURE	v
ACKNOWLEDGMENTS	vi
ABSTRACT	vii
CHAPTER 1. INTRODUCTION	1
1.1 Research Objectives	1
1.2 Investigated Drag Laws	1
CHAPTER 2. METHODOLOGY	4
2.1 Analytical Methodology	4
2.2 Numerical Methodology	5
CHAPTER 3. ANALYSIS OF DRAG CORRELATIONS	7
3.1 Validation of Implementation of Correlations	7
3.2 Results	8
CHAPTER 4. ANALYSIS OF DNS DATA	16
4.1 Validation of Quantity of Subdivisions	16
4.2 Results	18
4.3 Comparison of Mean and Local Volume Fraction Fluctuations	23
CHAPTER 5. CONCLUSIONS	24
REFERENCES	26
APPENDIX. MATLAB CODE	27

LIST OF FIGURES

Figure 3.1	Exchange coefficient predicted by Lundberg & Halvorsen [9].....	7
Figure 3.2	Drag predicted by correlations using MATLAB for conditions from Lundberg & Halverson [9].....	8
Figure 3.3	Predicted $\Delta FF\phi_0$ vs. $\Delta\phi$ for correlation proposed by Tenneti et al. [5] at varying Res and ϕ_0	9
Figure 3.4	Predicted $\Delta FF\phi_0$ vs. $\Delta\phi$ for correlation proposed by Beetstra et al. [3] at varying Res and ϕ_0	10
Figure 3.5	Predicted $\Delta FF\phi_0$ vs. $\Delta\phi$ for correlation proposed by Syamlal & O'Brien [1] at varying Res and ϕ_0	11
Figure 3.6	Predicted $\Delta FF\phi_0$ vs. $\Delta\phi$ for correlation proposed by Gidaspow [2] at varying Res and ϕ_0	12
Figure 3.7	Predicted $\Delta FF\phi_0$ vs. $\Delta\phi$ for correlation proposed by Zaidi et al. [7] at varying Res and ϕ_0	13
Figure 3.8	Predicted $\Delta FF\phi_0$ vs. $\Delta\phi$ for correlation proposed by Tang et al. [6] at varying Res and ϕ_0	14
Figure 3.9	Predicted $\Delta FF\phi_0$ vs. $\Delta\phi$ for correlation proposed by Bogner et al. [4] at varying Res and ϕ_0	15
Figure 4.1	Evaluation of varying subdivisions for $Res = 100$ and $\phi = 0.1$	17
Figure 4.2	Evaluation of varying subdivisions for $Res = 0.01$ and $\phi = 0.1$	18
Figure 4.3	$\Delta F'F$ with respect to $\Delta\phi$ for $\phi = 0.1$	19
Figure 4.4	$\Delta F'F$ with respect to $\Delta\phi$ for $\phi = 0.2$	20
Figure 4.5	$\Delta F'F$ with respect to $\Delta\phi$ for $\phi = 0.3$	21
Figure 4.6	$\Delta F'F$ with respect to $\Delta\phi$ for $\phi = 0.4$	22

LIST OF TABLES

Table 1.1	Evaluated drag laws.....	3
Table 3.1	Parameters for drag law verification	7

NOMENCLATURELatin Letters

F	Drag force per volume (N/m^3)
Re_s	Slip Reynolds number
d	Particle diameter (m)
u_f	Fluid velocity (m/s)
C_D	Coefficient of drag
C_g	Coefficient of growth

Greek Letters

ϕ	Solid volume fraction
ρ	Fluid density (kg/m^3)
v_r	Relative velocity correlation
μ	Fluid viscosity ($kg/m \cdot s$)
Δ	Change in value

Subscripts & Superscripts

\bar{x}	Mean value
x_0	Initial value
x^*	Non-dimensional value
x'	Local value

ACKNOWLEDGMENTS

I would like to thank my committee chair, Dr. Passalacqua, and my committee members, Dr. Fox and Dr. Subramaniam, for the assistance and guidance they have offered throughout my time at Iowa State University. I would also like to thank Dr. Ganapathysubramanian for serving as a substitute committee member during my defense in the absence of Dr. Fox.

In addition, I would also like to thank Vahid Tavanashad for helping me use Subramaniam group's PUREIBM code and being very patient with all my questions on it. Lastly, I would to thank the members of Beta Sigma Psi and the Iowa State Quidditch Club for making my time outside of academics all the more memorable.

ABSTRACT

This thesis presents the results of an analysis of the effect of changes in the mean volume fraction and local volume fraction have on the drag force in flow past a fixed assembly of spheres. Current drag correlations address the mean drag of the system, but neglect changes in the mean and local volume fraction which could affect the flow more locally. The impact to the local drag and mean system drag, from local and mean volume fraction changes respectively, are compared. This is done by finding the predicted change in mean drag force as the mean volume fraction of the system changes for a variety of drag laws and comparing it with data from simulations in which the local drag and volume fraction fluctuations can be extracted. These simulations were previously performed using the PReIBM method. It will be shown the local drag does not show a clear correlation in regard to local volume fraction changes. Furthermore, it will be seen the local drag fluctuations are negligible compared to the mean drag changes from a mean volume fraction change in the system.

CHAPTER 1. INTRODUCTION

1.1 Research Objectives

There are numerous correlations which are used to describe particulate flow. Syamlal & O'Brien [1] propose a correlation based on the principle the Archimedes number remains the same for both a single particle and a system of particles. They use this to create a correlation between the settling velocity for a single particle and for a system, which is then used to modify the drag of a single particle to obtain the drag for a system. Gidaspow [2] suggests a combination of the Wen & Yu correlation and the Ergun equation, using Wen & Yu in the dilute region while using Ergun when the system is more packed. Beetstra et al. [3] and Bogner et al. [4] propose correlations based on simulated flow past an assembly of spheres using the Lattice-Boltzmann method. Tenneti et al. [5], Tang et al. [6], and Zaidi et al. [7] use an Immersed Boundary Method to simulate flow past an assembly of particles, each proposing a correlation based on their results. These correlations are for predicting the mean drag of the system, and as such use the mean volume fraction of the system. It is possible, however, for there to be fluctuations in the local volume fraction of an overall homogenous dispersion of particles. The purpose of this work is to investigate whether this change in local volume fraction produces appreciable changes in the local drag, and to develop a correlation for these fluctuations. It is also investigated as to how these fluctuations compare to the predicted change in mean drag from a change in the mean volume fraction of the system.

1.2 Investigated Drag Laws

In this work, seven drag correlations are analyzed: Tenneti et al. [1], Beetstra et al. [2], Zaidi et al. [3], Bogner et al. [4], Tang et al. [5], Gidaspow [6], and Syamlal & O'Brien [7]. Table 1.1 shows each drag correlation as implemented in this work, the form in which it was

initially reported, and any scaling factor used in the initial form. The final form of the correlation is for flow past a fixed assembly of particles, where the particle velocity is zero. Due to this, only the fluid velocity, u_f , is used.

The initial form of the correlations can take two forms, mean force per particle or mean force per volume. Following the notation of Mehrabadi [8], the first case will be denoted with $\langle \mathbf{F}_h \rangle$ while the second will be denoted as $\langle \mathbf{f}_h \rangle$. The second form is the desired form for this work, and it will be shown later how to convert between the two.

For this work, the scaling factor is defined to be a term which is used to normalize the value by a reference point and put the output in non-dimensional form as shown in Eqn. 1.1.

$$F^* = \frac{F}{F_{scaling}} \quad (1.1)$$

Table 1.1 Evaluated drag laws

Drag Law	Initial Form	Scaling Factor	Implemented Form
Tenneti et al.	$\langle \mathbf{F}_h \rangle$	Stokes Drag	$F = \left[\frac{1 + 0.15Re_s^{0.687}}{(1-\phi)^3} + \frac{5.81\phi}{(1-\phi)^3} + 0.48 \frac{\phi^{1/3}}{(1-\phi)^4} + \phi^3 Re_s \left(0.95 + \frac{0.61\phi^3}{(1-\phi)^2} \right) \right] \frac{6\phi}{\pi d^3} F_{st}$
Beetstra et al.	$\langle \mathbf{F}_h \rangle$	Stokes Drag	$F = \left[\frac{10\phi}{(1-\phi)^3} + (1-\phi)(1 + 1.5\sqrt{\phi}) + \frac{0.413Re_s}{24(1-\phi)^3} \left(\frac{(1-\phi)^{-1} + 3\phi(1-\phi) + 8.4Re_s^{-0.343}}{1 + 10^3\phi Re_s^{-(1+4\phi)/2}} \right) \right] \frac{6\phi}{\pi d^3} F_{st}$
Syamlal & O'Brien	$\langle \mathbf{f}_h \rangle$	None	$F = \frac{3\phi(1-\phi)\rho}{4dv_r^2} C_D u_f^2$ $C_D = \left[0.63 + \frac{4.8}{\sqrt{\frac{Re_s}{v_r}}} \right]^2$ $v_r = \frac{1}{2} [A - 0.06Re_s] + \frac{1}{2} \left[\sqrt{(0.06Re_s)^2 + 0.12Re_s(2B - A) + A^2} \right]$ $A = (1-\phi)^{4.14}$ $B = \begin{cases} 0.8(1-\phi)^{1.28} & \phi \geq 0.15 \\ (1-\phi)^{2.65} & \phi < 0.15 \end{cases}$
Gidaspow	$\langle \mathbf{f}_h \rangle$	None	$F_{Wen \& Yu} = \frac{3\rho(1-\phi)\phi}{4d} C_D u_f^2 (1-\phi)^{-2.65}$ $C_D = \frac{24}{Re_s} \left[1 + 0.15Re_s^{0.687} \right]$ $F_{Ergun} = \left[150 \frac{\mu\phi^2}{(1-\phi)d^2} + 1.75 \frac{\rho u_f \phi}{d} \right] u_f$ $F = \begin{cases} F_{Wen \& Yu}, & \phi < 0.2 \\ F_{Ergun}, & \phi \geq 0.2 \end{cases}$
Zaidi et al.	$\langle \mathbf{F}_h \rangle$	Stokes Drag	$F = \begin{cases} \left[\frac{10\phi}{(1-\phi)^3} + (1-\phi)(1 + 1.5\sqrt{\phi}) + \frac{0.0034}{(1-\phi)^{3.7}} Re_s \right] \frac{6\phi}{\pi d^3} F_{st} & Re_s \leq 200 \\ \left[\frac{10.9\phi^{0.4}}{(1-\phi)^{2.7}} + \frac{0.024}{(1-\phi)^{3.86}} Re_s \right] \frac{6\phi}{\pi d^3} F_{st} & Re_s > 200 \end{cases}$
Tang et al.	$\langle \mathbf{F}_h \rangle$	Stokes Drag	$F = \left[\frac{10\phi}{(1-\phi)^3} + (1-\phi)(1 + 1.5\sqrt{\phi}) + \frac{Re_s}{1-\phi} \left(0.11\phi(1-\phi) - \frac{0.00456}{(1-\phi)^4} + \left(0.169(1-\phi) + \frac{0.0644}{(1-\phi)^4} \right) Re_s^{-0.343} \right) \right] \frac{6\phi}{\pi d^3} F_{st}$
Bogner et al.	$\langle \mathbf{F}_h \rangle$	Stokes Drag	$F = \left[(1-\phi)^{-5.726} (1.751 + 0.151Re_s^{0.684} - 0.445(1 + Re_s)^{1.04\phi} - 0.16(1 + Re_s)^{0.0003\phi}) \right] \frac{6\phi}{\pi d^3} F_{st}$

CHAPTER 2. METHODOLOGY

2.1 Analytical Methodology

Investigation into the effect a change in the mean volume fraction has on the mean drag will be done analytically with MATLAB. To compare the predicted drag to the numerical data, the result must be given as mean force per volume. The correlations, in the forms presented by Lundberg & Halvorsen [9] and Akiki et al. [10], are given as a momentum exchange coefficient or mean force per particle, respectively. For the first form, simply multiplying the correlation by the slip velocity yields the mean force per volume. For the second form, Eqn. 2.1, from Mehrabadi [8], can be used to convert from mean force per particle to mean force per volume.

$$\langle \mathbf{f}_h \rangle = \langle \mathbf{F}_h \rangle \frac{6\bar{\phi}}{\pi d^3} \quad (2.1)$$

In addition to this, the correlations must be multiplied by any normalizing factor present. The correlations presented by Akiki et al. are all normalized by Stokes drag, as defined by Eqn. 2.2, and so are multiplied by that term. Those presented by Lundberg & Halvorsen have no normalizing factor.

$$F_{Stokes} = 3\pi\mu d(1 - \bar{\phi})u_f \quad (2.2)$$

The Reynolds number used in these drag laws is the slip Reynolds number, which is defined by Eqn. 2.3. By holding the slip Reynolds number constant, Eqn. 2.3 can be rearranged to solve for the fluid velocity based on the local volume fraction. From here onwards, the slip Reynolds number will be referred to simply as the Reynolds number.

$$Re_s = \frac{\rho d(1-\phi)u_f}{\mu} \quad (2.3)$$

The predicted change in mean drag force, $\Delta\bar{F}$, due to change in mean volume fraction, $\Delta\bar{\phi}$, is found by Eqn. 2.4.

$$\Delta\bar{F} = \bar{F}(\bar{\phi} + \Delta\bar{\phi}) - \bar{F}(\bar{\phi}) \quad (2.4)$$

This assumes the rate of change of \bar{F} is dependent solely on the rate of change of $\bar{\phi}$ and has constant gradient.

2.2 Numerical Methodology

To investigate how fluctuations in the local volume fraction affect local drag, existing data, from Mehrabadi [8], will be analyzed. He used a direct numerical simulation (DNS) method called Particle-resolved Uncontaminated-fluid Reconcilable Immersed Boundary Method (PUREIBM), developed by Dr. Subramaniam's group at Iowa State University. It gets its name through its unique immersed boundary forcing implementation. The boundary forcing required to enforce the no-slip and no-penetration condition of the particles is only present in the nodes within the particle, keeping the fluid phase uncontaminated. This enables the drag force for each particle to be computed by integrating the stress tensor over the surface of the particle. The governing equations are solved on a Cartesian grid with periodic boundary conditions. Thorough documentation can be found in previous articles [11, 12].

For this work, the post-processing portion of PUREIBM was altered by Dr. Subramaniam's group to allow for the subdivision of the simulation domain in to smaller sections when evaluating data from previous simulations. The drag force and volume fraction of each of these subdivisions will be referred to as *local values*. The mean volume fraction for each realization will be the total volume fraction of the domain, and the mean drag is the total drag force of the entire domain. The fluctuations between the mean volume fraction and

local volume fraction is found using Eqn. 2.4. Force fluctuations are found in the same manner.

$$\Delta\phi = \phi' - \bar{\phi} \quad (2.5)$$

The setup evaluated for this work is flow past a fixed random assembly of spheres [8]. The simulations cover a range of Re_s from 0.01-100 and $\bar{\phi}$ from 0.1-0.4. For each combination of Re_s and $\bar{\phi}$, five realizations were evaluated.

CHAPTER 3. ANALYSIS OF DRAG CORRELATIONS

3.1 Validation of Implementation of Correlations

Once the selected drag correlations were in MATLAB, they were validated against results from Lundberg & Halvorsen [9], which showed predicted drag for gas flow past an assembly of spheres. Table 3.1 shows the setup parameters for the validation case.

Table 3.1 Parameters for drag law verification

d	154 μm
ρ	1.225 kg / m^3
μ	1.7894x10 ⁻⁵ $\text{kg} / \text{m}\cdot\text{s}$
Re_s	1.4

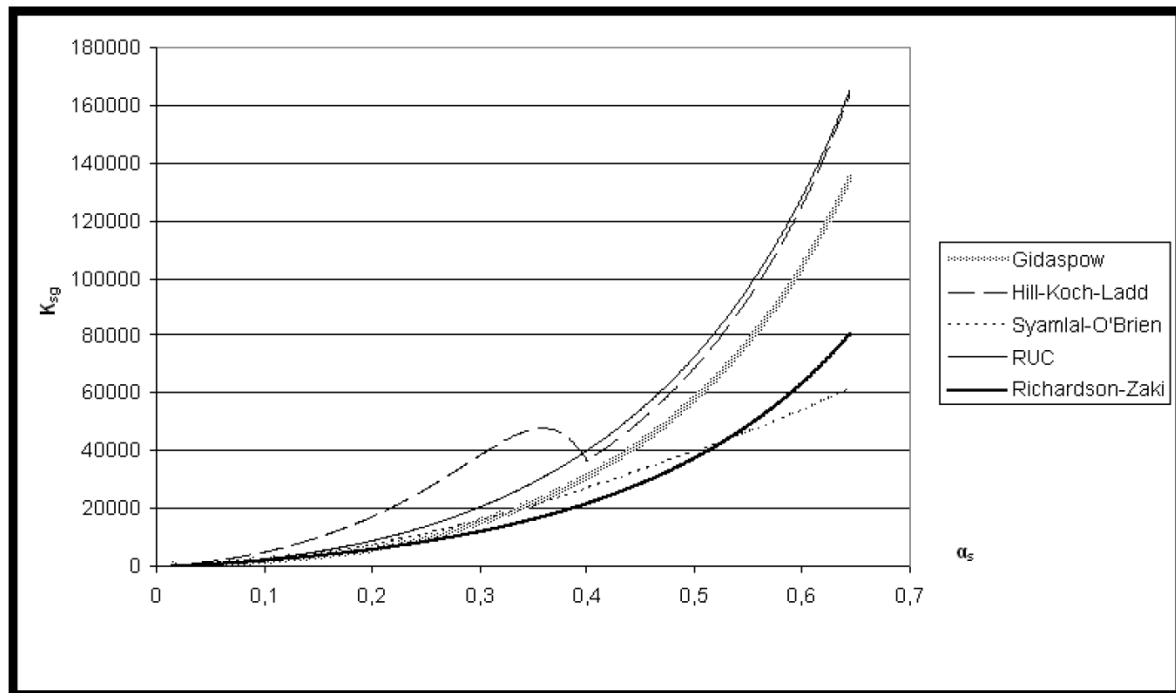


Figure 3.1 Exchange coefficient predicted by Lundberg & Halvorsen [9]

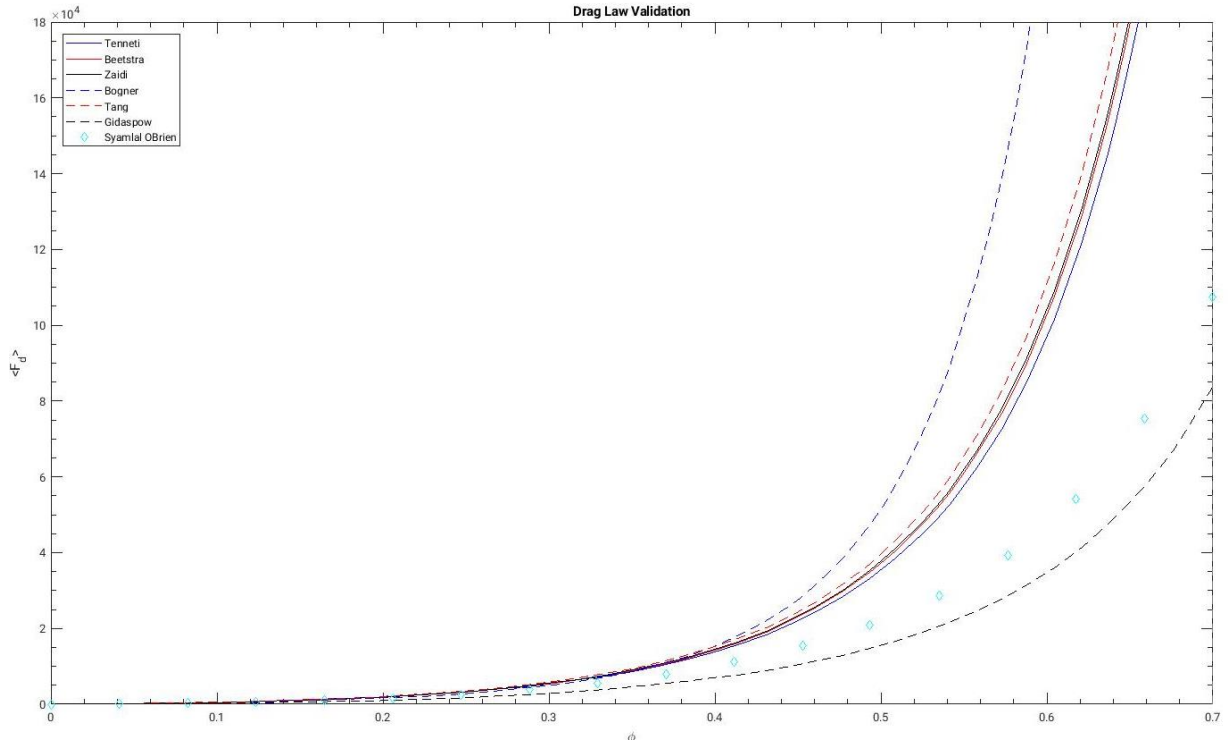


Figure 3.2 Drag predicted by correlations using MATLAB for conditions from Lundberg & Halverson [9]

The discrepancy in the magnitudes is due to the difference in what is being reported. In the literature it is being reported as a momentum exchange coefficient, while the MATLAB results are in mean force per volume. The conversion from the first form to the second is achieved by multiplying by the slip velocity, which in this case is just the fluid velocity due to the particles being fixed. This value is the same for all the cases, and so although the magnitude changes the overall trends should stay the same. It is seen the results from MATLAB follow the same trends, which suggests they have been properly implemented.

3.2 Results

The graphs following show the results from MATLAB, evaluating the change in mean drag force. The vertical axis shows the change in mean drag force normalized by the

mean drag force at the initial mean volume fraction. The horizontal axis shows the change in mean volume fraction, with 0 representing the initial mean volume fraction. There are four graphs for each drag correlation, one for each of the initial mean volume fractions, and each one contains each Reynolds number evaluated. Due to the Gidaspow correlation being piecewise in nature, and as such discontinuous at a volume fraction of 0.2, a volume fraction of 0.201 was used instead for evaluation.

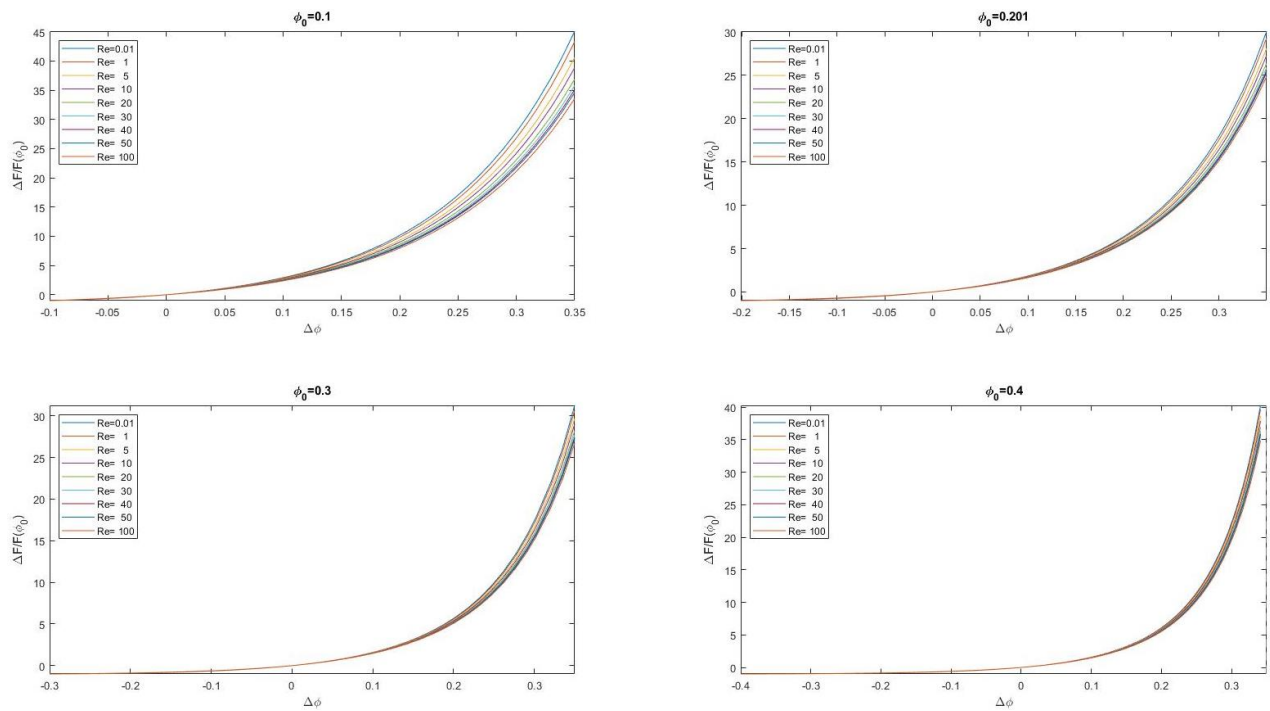


Figure 3.3 Predicted $\Delta \bar{F} / \bar{F}(\bar{\phi}_0)$ vs. $\Delta \bar{\phi}$ for correlation proposed by Tenneti et al. [5] at varying Re_s and $\bar{\phi}_0$

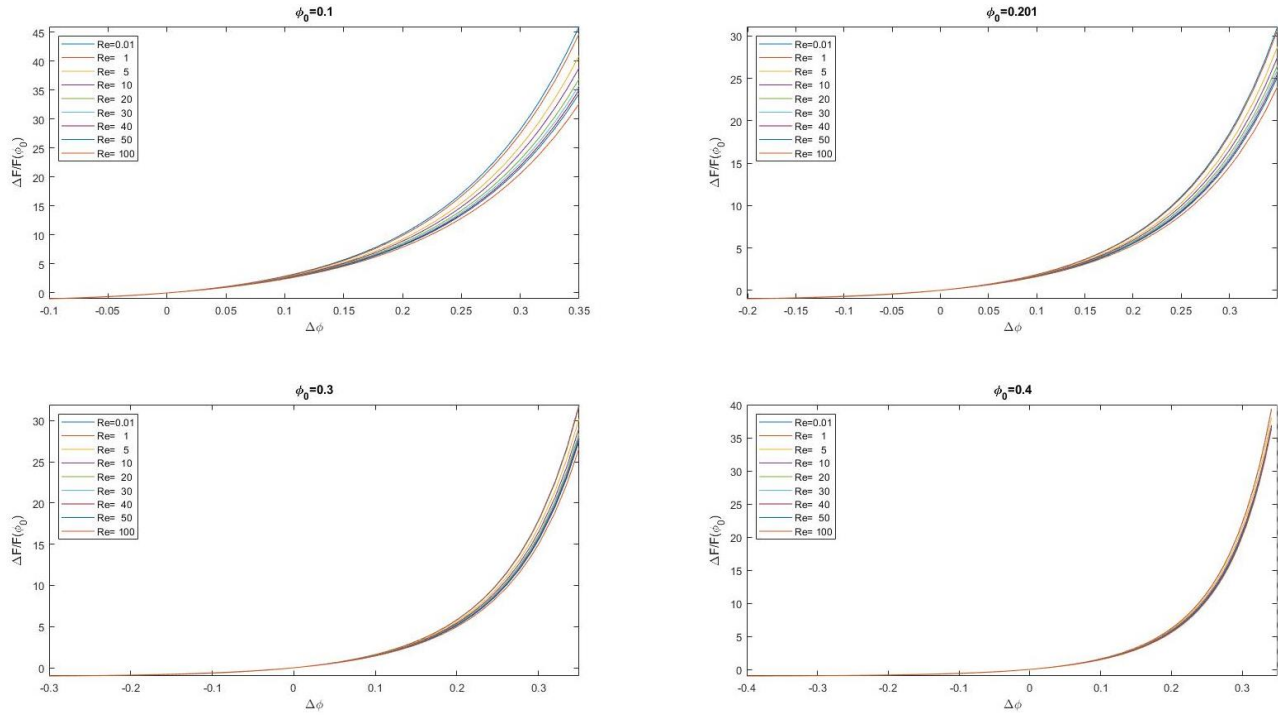


Figure 3.4 Predicted $\Delta \bar{F} / \bar{F}(\bar{\phi}_0)$ vs. $\Delta \bar{\phi}$ for correlation proposed by Beetstra et al. [3] at varying Re_s and $\bar{\phi}_0$

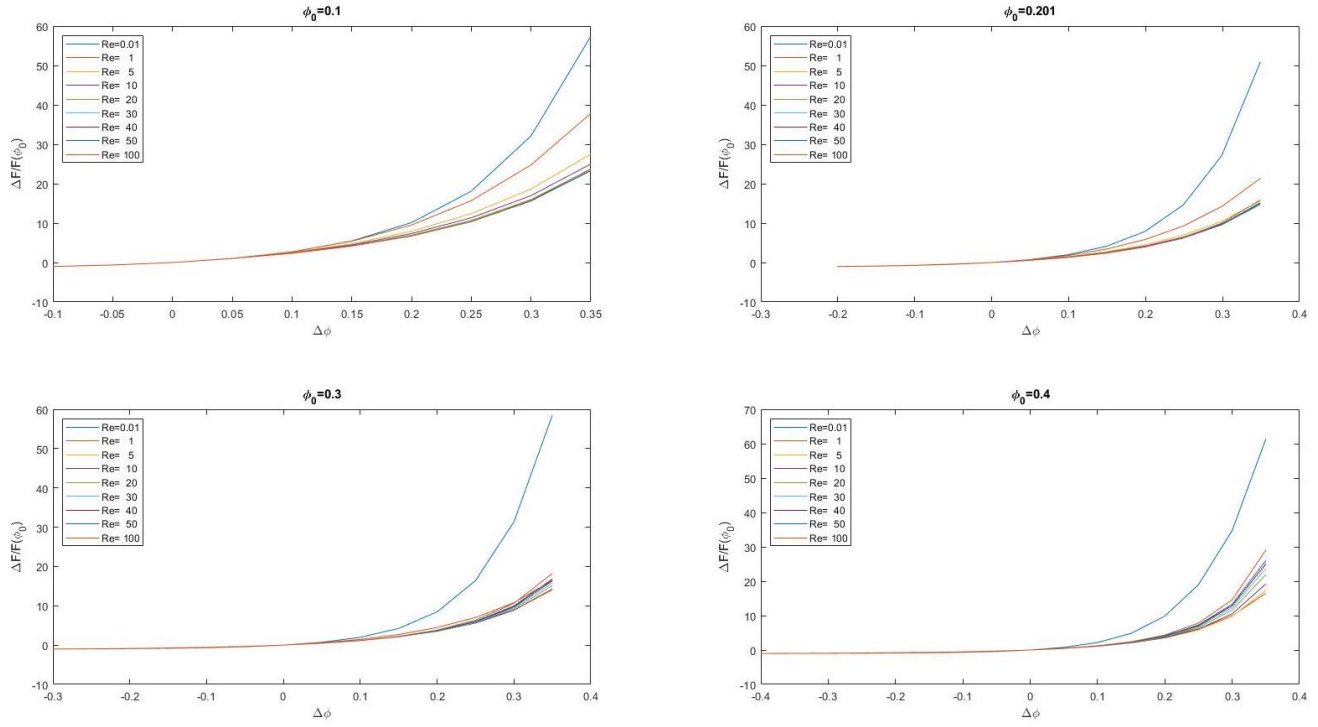


Figure 3.5 Predicted $\Delta \bar{F} / \bar{F}(\bar{\phi}_0)$ vs. $\Delta \bar{\phi}$ for correlation proposed by Syamlal & O'Brien

[1] at varying Re_s and $\bar{\phi}_0$

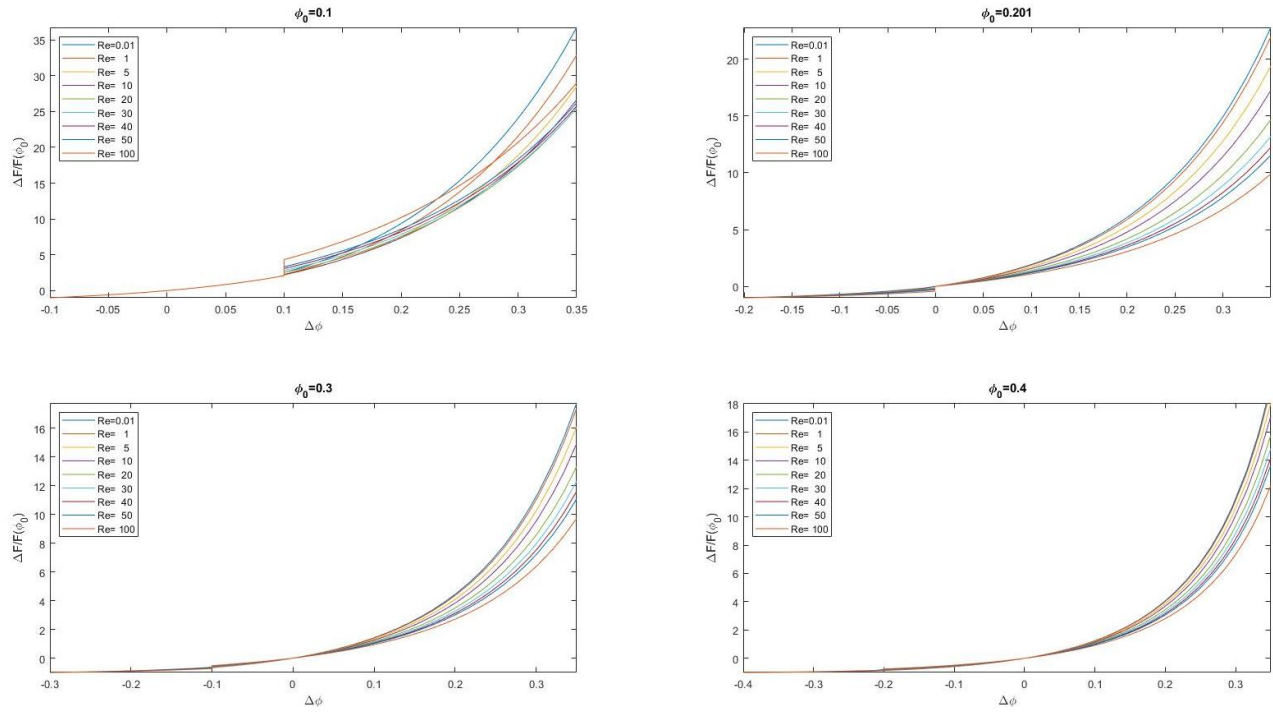


Figure 3.6 Predicted $\Delta \bar{F} / \bar{F}(\bar{\phi}_0)$ vs. $\Delta \bar{\phi}$ for correlation proposed by Gidaspow [2] at varying Re_s and $\bar{\phi}_0$

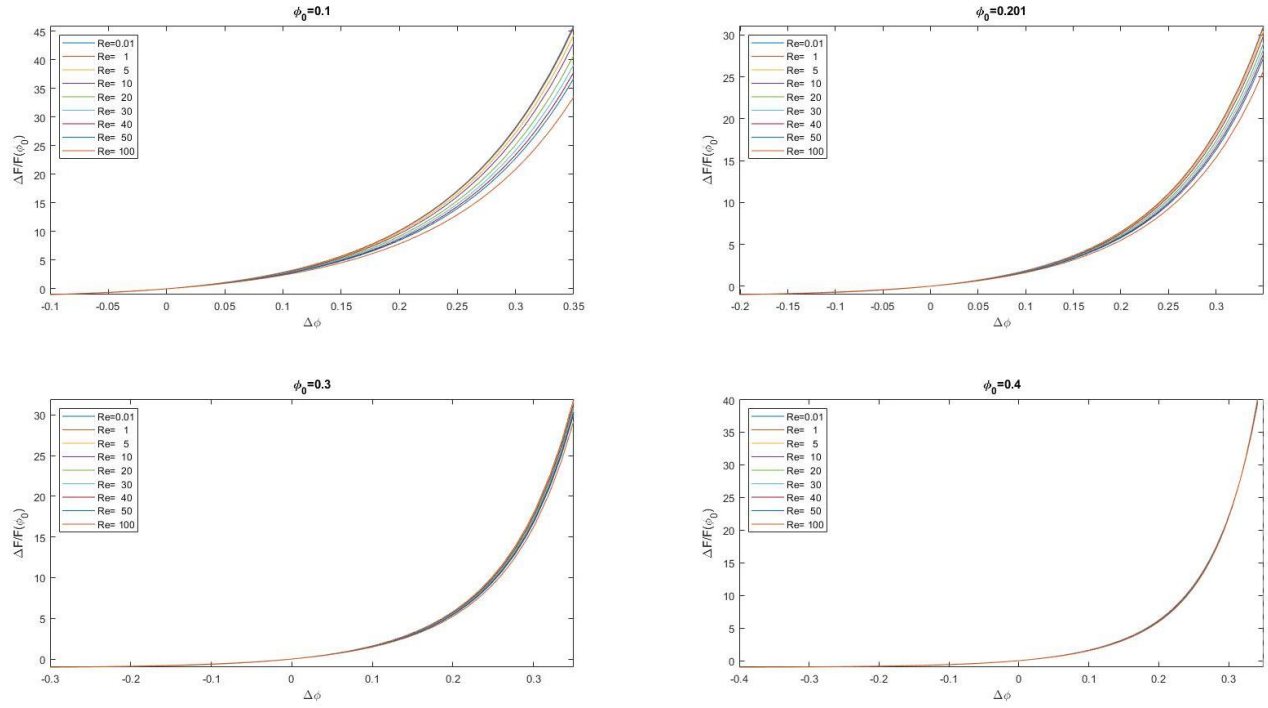


Figure 3.7 Predicted $\Delta \bar{F} / \bar{F}(\bar{\phi}_0)$ vs. $\Delta \bar{\phi}$ for correlation proposed by Zaidi et al. [7] at varying Re_s and $\bar{\phi}_0$

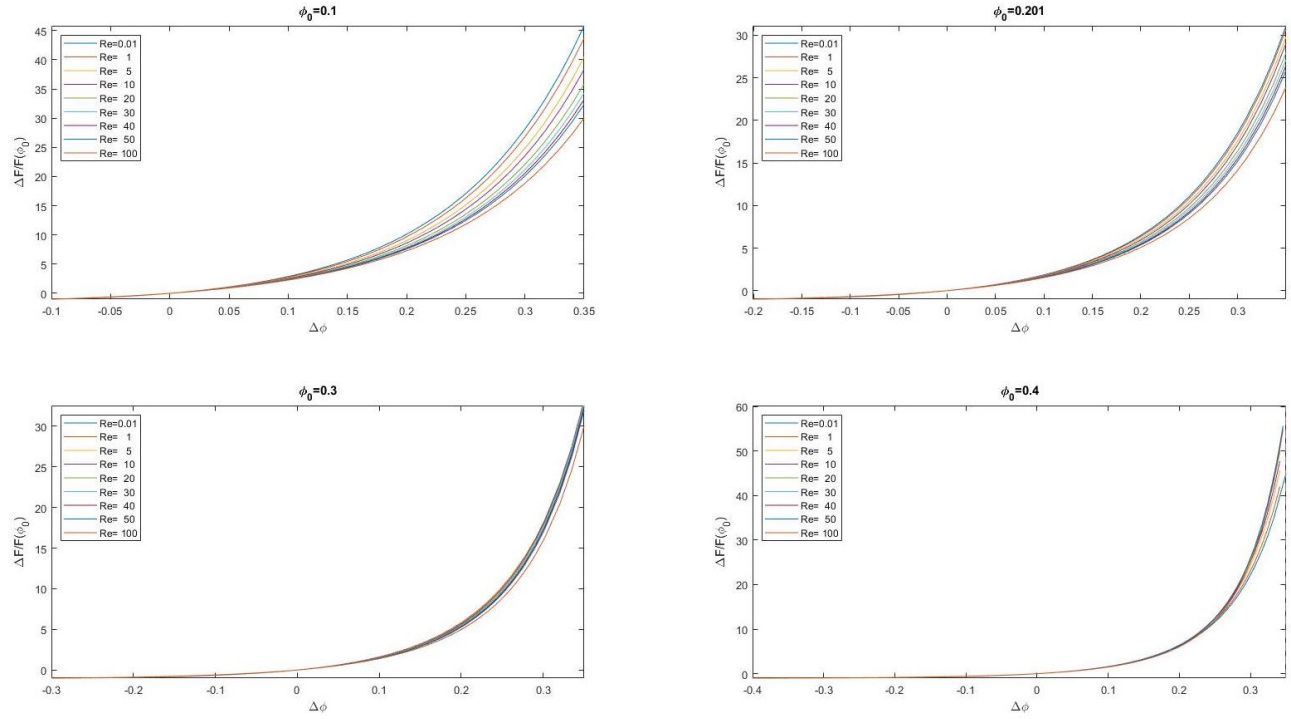


Figure 3.8 Predicted $\Delta \bar{F} / \bar{F}(\bar{\phi}_0)$ vs. $\Delta \bar{\phi}$ for correlation proposed by Tang et al. [6] at varying Re_s and $\bar{\phi}_0$

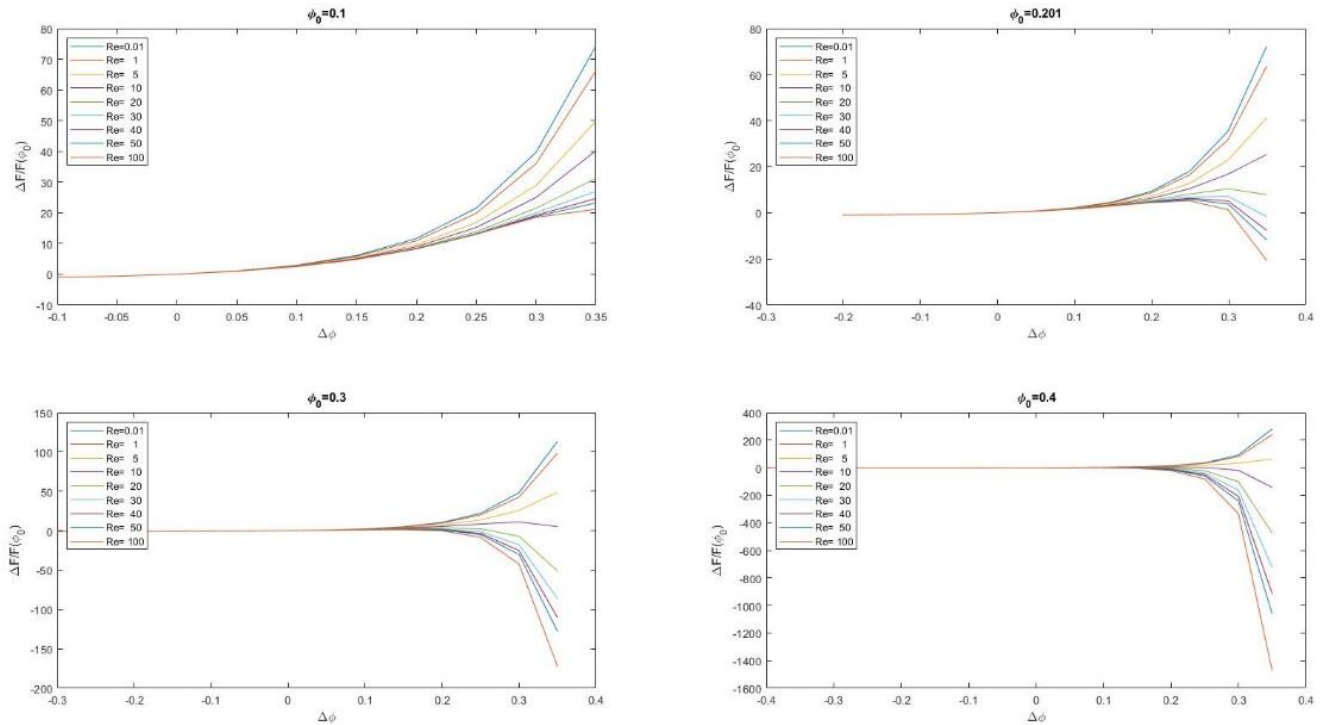


Figure 3.9 Predicted $\frac{\Delta \bar{F}}{\bar{F}(\bar{\phi}_0)}$ vs. $\Delta \bar{\phi}$ for correlation proposed by Bogner et al. [4] at varying Re_s and $\bar{\phi}_0$

The behavior of the drag laws, for a change in the $\bar{\phi}$, generally follows a similar trend. They tend to have the form of an exponential curve, with varying degrees of steepness and magnitude. The notable outlier are the results for Bogner et al., which trend very steeply downwards for higher volume fractions for most Reynolds numbers. This is most likely due to the correlation of Bogner et al. not being valid for $\phi > 0.35$ [4]. Overall, these results seem reasonable based on the results from Figure 3.2. There we see an exponential growth, so it seems reasonable the growth of the differences would follow a similar trend.

CHAPTER 4. ANALYSIS OF DNS DATA

4.1 Validation of Quantity of Subdivisions

To determine the effect a fluctuation in local volume fraction (ϕ') has on the local drag force (F'), cases by Mehrabadi [8] will be evaluated. These are simulations of flow past a random fixed assembly of spheres using PReIBM. For these, $\bar{\phi}$ will be defined as the volume fraction of the entire domain while \bar{F} is $F(\bar{\phi})$, or the total drag force in the domain. Local values will be calculated by splitting the domain in to equally sized subdivisions and finding F' and ϕ' for each. The fluctuations are then found using Eqn. 2.5.

The smallest amount of subdivisions is one, which results in the domain average, and the most would be dependent on the particle size. If subdivisions were small enough such that the length of one side of the subdivision was smaller than the particle diameter, you could evaluate a subdivision entirely within a particle. For $Re_s = 0.01$ and $Re_s = 100$, with $\bar{\phi} = 0.1$, a range of subdivisions was tested. Figures 4.1 and 4.2 show the results of these tests.

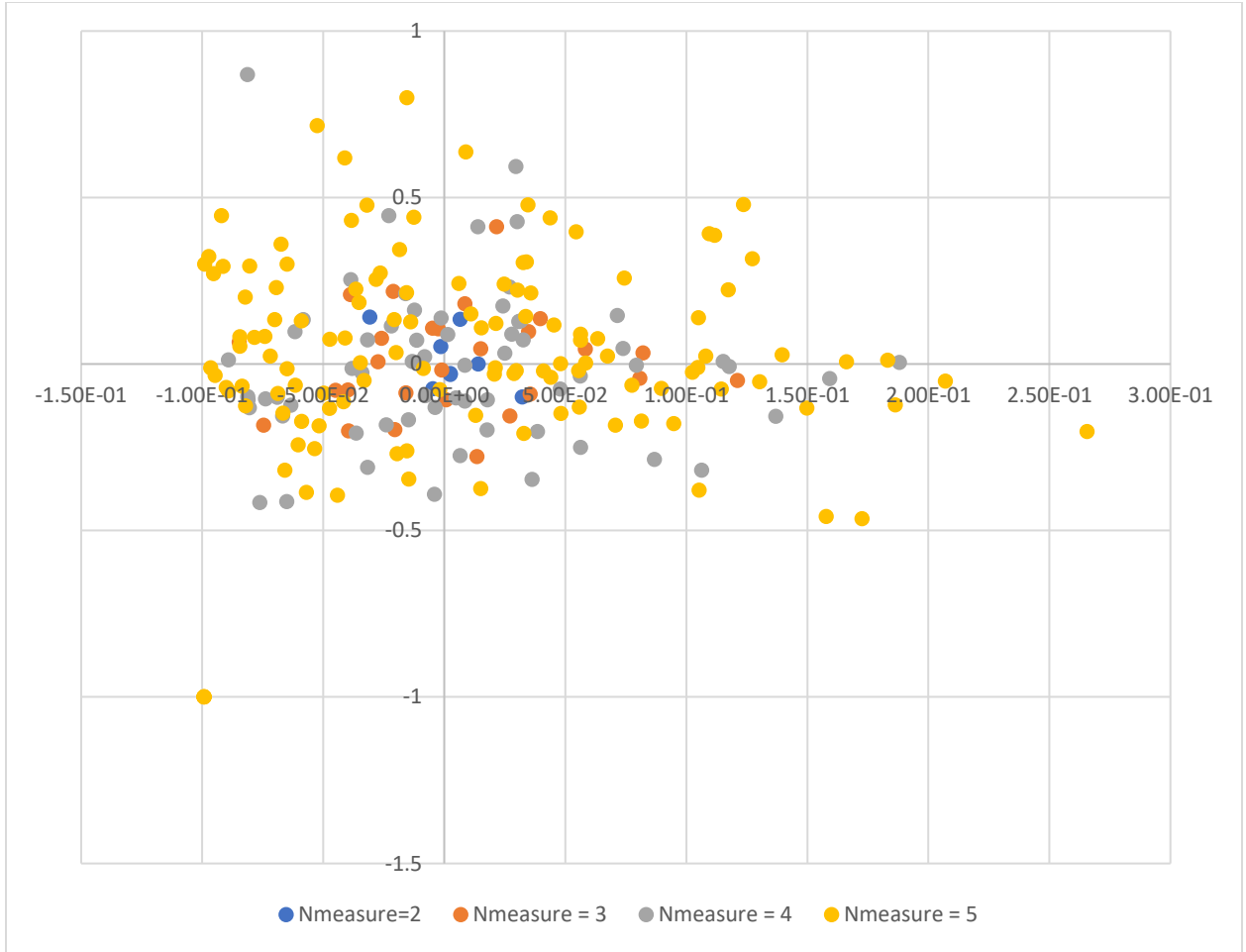


Figure 4.1 Evaluation of varying subdivisions for $Re_s = 100$ and $\bar{\phi} = 0.1$

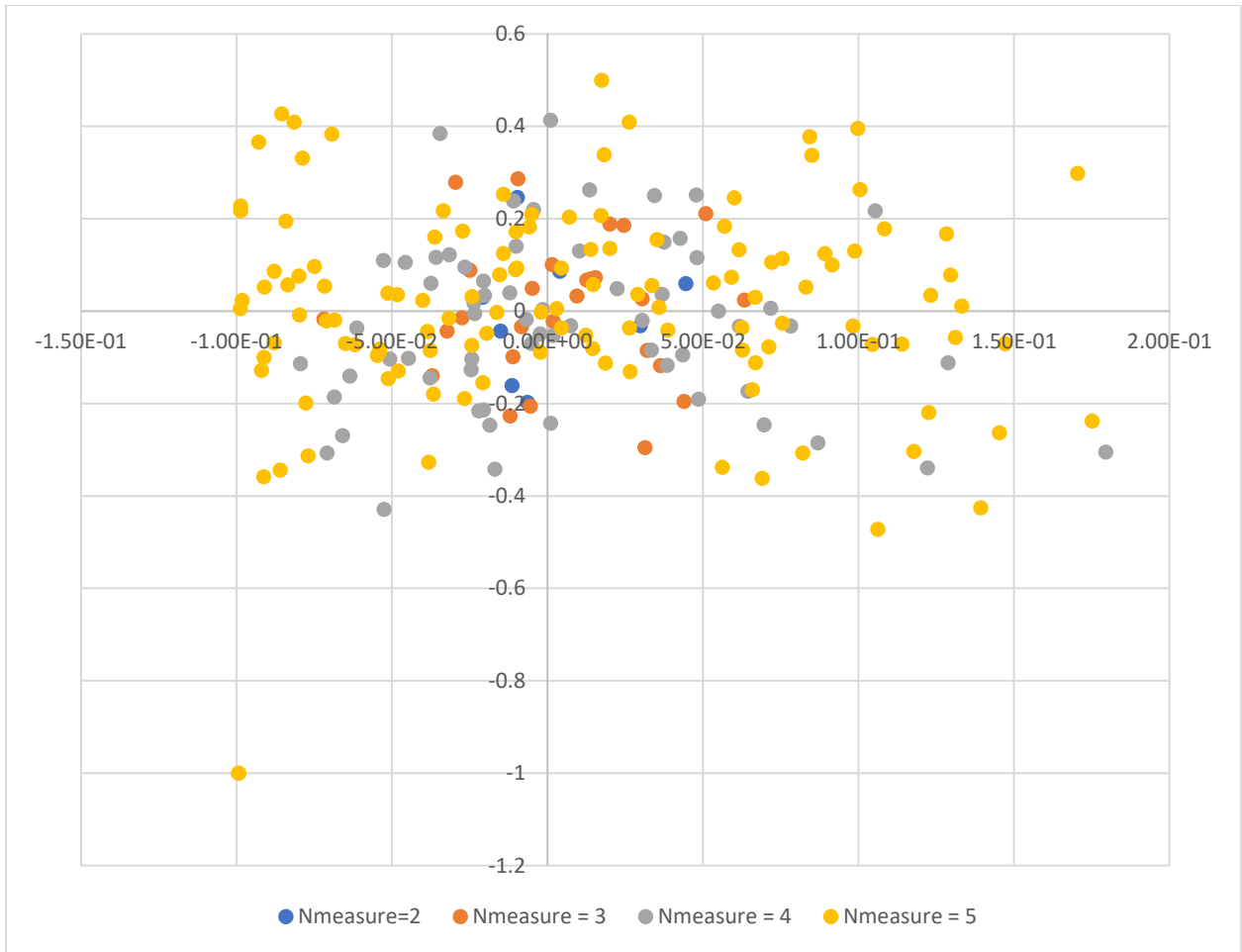


Figure 4.2 Evaluation of varying subdivisions for $Re_s = 0.01$ and $\bar{\phi} = 0.1$

It does not appear to make a difference whether a small or large number of subdivisions are used, the results do not show a clear trend regardless. For this work, 125 subdivisions were used to allow the analysis of the more extreme fluctuations to get a better idea of the range of drag fluctuations.

4.2 Results

Figures 4.3-4.6 show the results from the evaluation of the data from Mehrabadi [8]. In each of these, the horizontal axis is the volume fraction fluctuation and the vertical axis is the drag force fluctuation divided by the mean drag force.

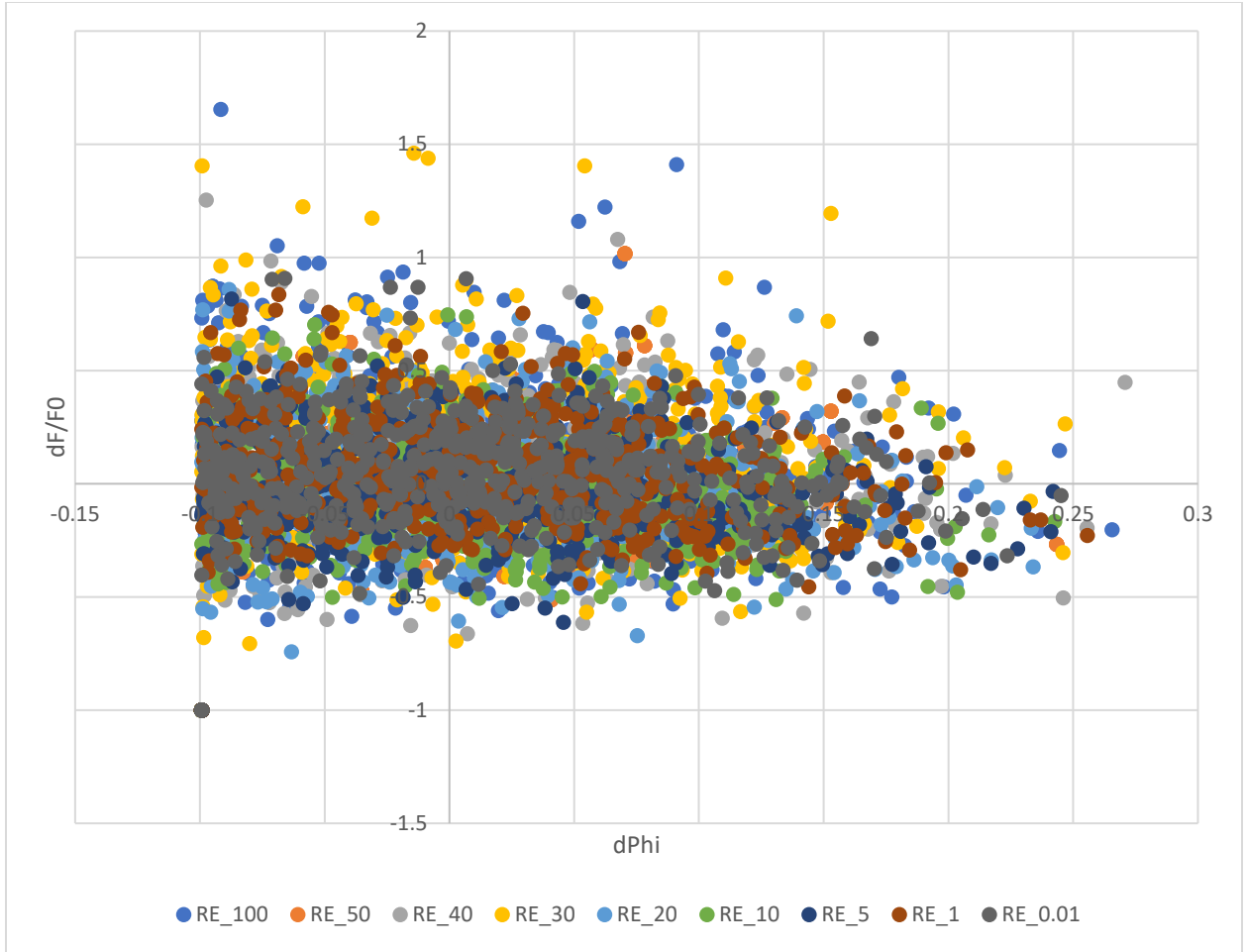


Figure 4.3 $\Delta F'/\bar{F}$ with respect to $\Delta\phi$ for $\bar{\phi} = 0.1$

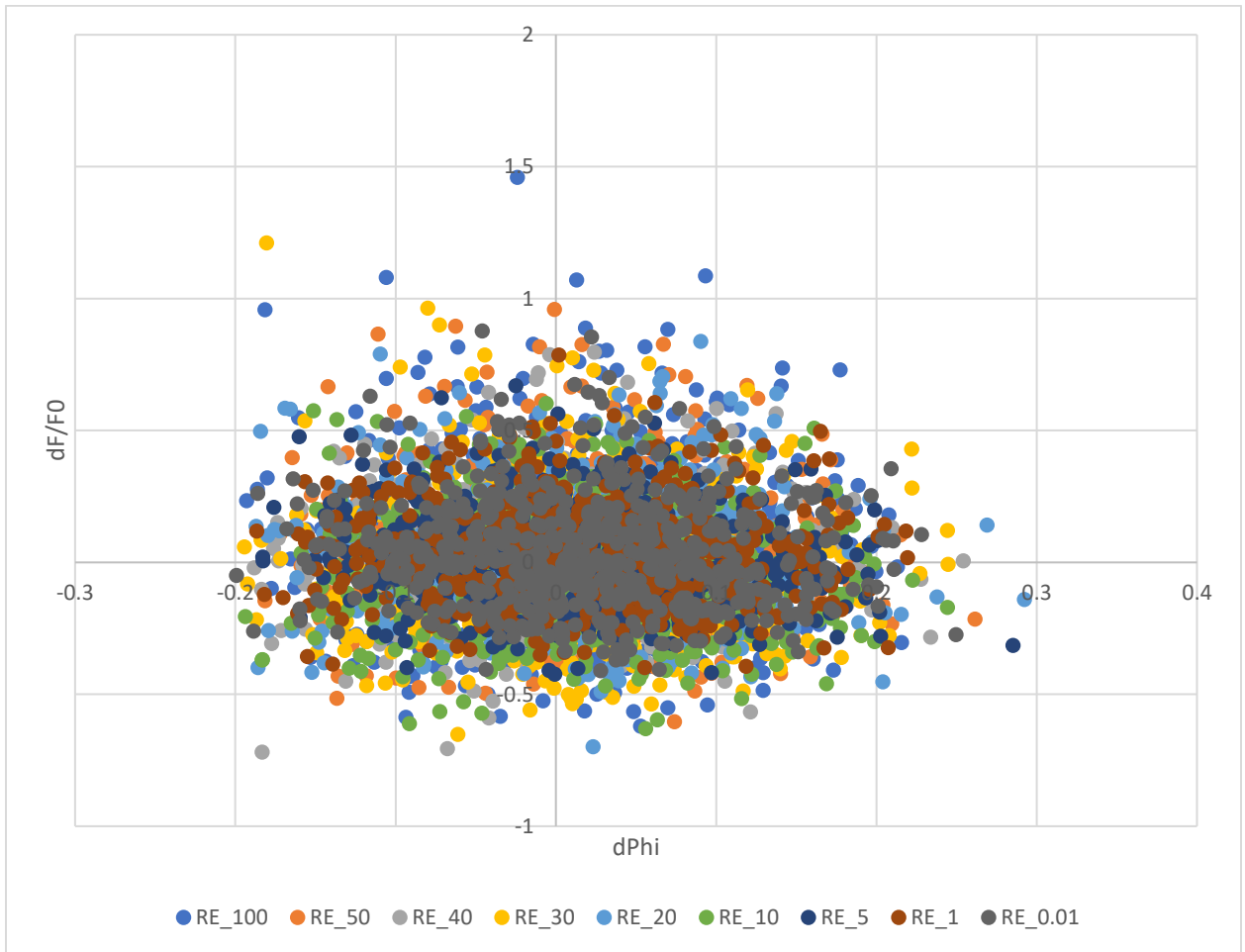


Figure 4.4 $\Delta F'/\bar{F}$ with respect to $\Delta\phi$ for $\bar{\phi} = 0.2$

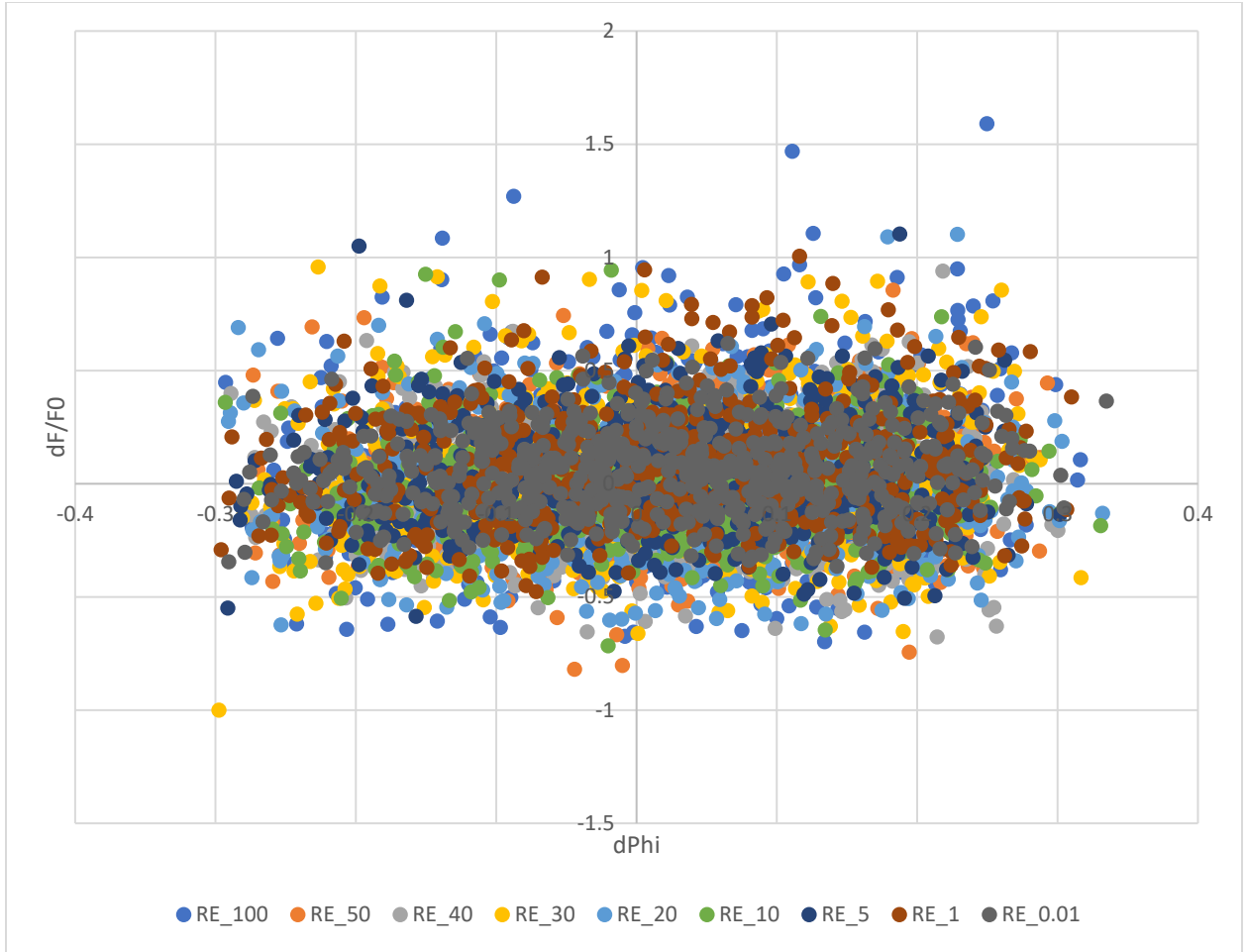


Figure 4.5 $\Delta F'/\bar{F}$ with respect to $\Delta\phi$ for $\bar{\phi} = 0.3$

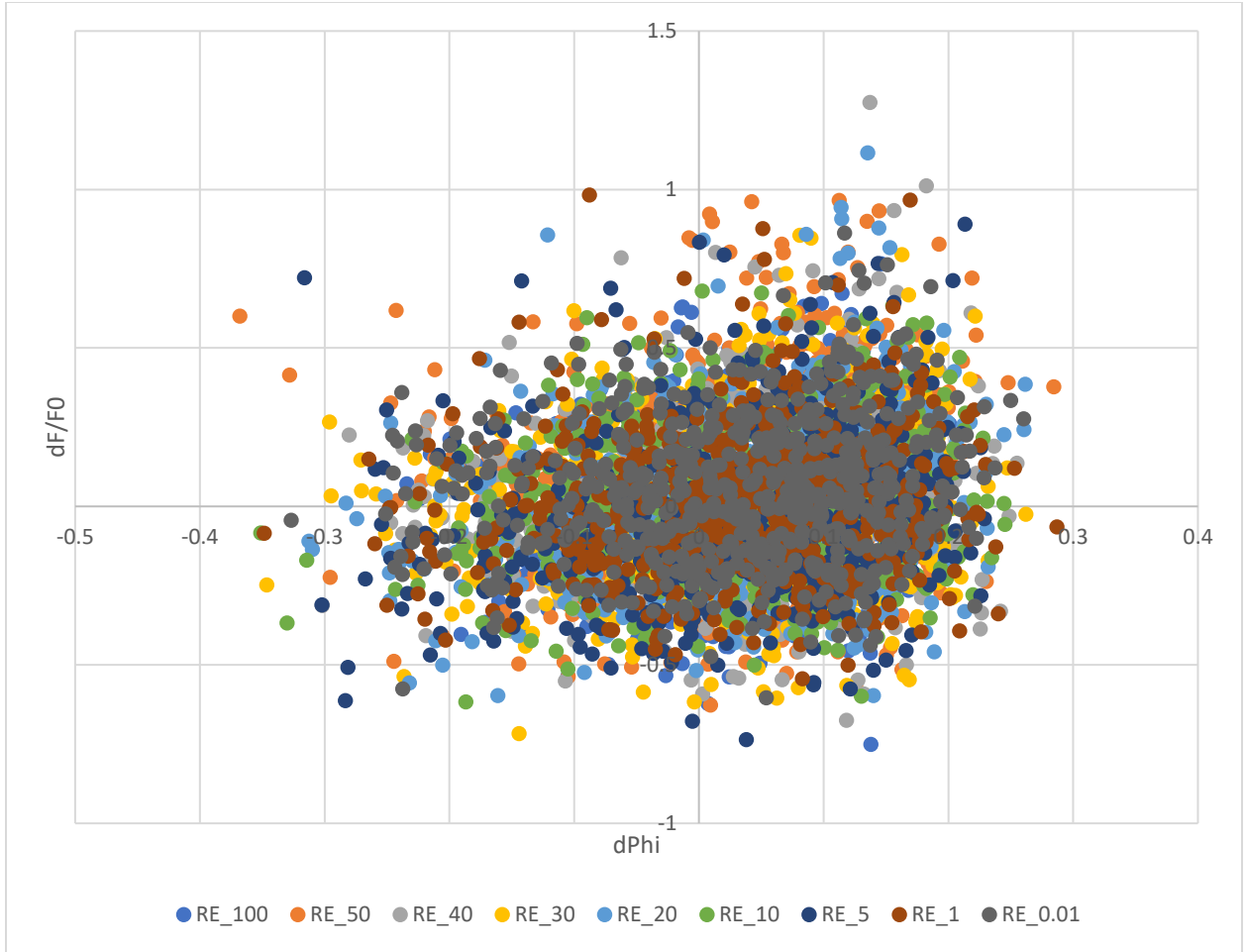


Figure 4.6 $\Delta F'/\bar{F}$ with respect to $\Delta\phi$ for $\bar{\phi} = 0.4$

Figure 4.3-4.6 all show $\Delta F'/\bar{F}$ having a completely random distribution. There is, however, one interesting thing worth pointing out, which is there seems to be no correlation between either Re_m or $\Delta\phi$ and $\Delta F'/\bar{F}$. Comparing the graphs, the bulk of each lies between $\Delta F'/\bar{F} = -0.5$ and $\Delta F'/\bar{F} = 0.5$, across all values of $\Delta\phi$. This implies, if there is some method for predicting local drag fluctuations, it would be fairly consistent across different flow conditions.

4.3 Comparison of Mean and Local Volume Fraction Fluctuations

When comparing the results from Chapter 4 and Chapter 3, the most immediately noted difference is the magnitude of the results. The results for $\Delta\bar{F}/\bar{F}(\phi_0)$ are many times larger than those for $\Delta F'/\bar{F}$. The other noteworthy difference is the distribution of data. The results for $\Delta F'/\bar{F}$ are random, while $\Delta\bar{F}/\bar{F}(\phi_0)$ was ordered.

Ultimately, the conclusions to be drawn from the comparison of the two, is that changes in $\bar{\phi}$ are far more impactful than changes in ϕ' . This implies the overall characteristics of a system are more meaningful than local variance in characteristics. In addition, it seems reasonable to neglect these local variances in most cases, which the drag laws investigated in this work do. Neglecting these variances help to simplify simulations, allowing you to treat a system as homogeneous using correlations based on average values.

The last observation is the ability to model, and therefore predict, the impact of the changes in volume fraction. The drag laws investigated, although developed in different ways, are all the product of modeling the effects of changes in mean volume fraction. The effect of changes to the local volume fraction does not show a clear trend and is not predictable solely with Reynolds number and $\Delta\phi$. Based on the results presented in Section 4.2, it appears the local drag fluctuations cannot be predicted, but possibly when related to different parameters a trend will emerge.

CHAPTER 5. CONCLUSIONS

There are three conclusions to draw from what has been presented. First, is the drag laws investigated predict similar trends for changes to mean volume fraction. The second is the behavior of the local drag due to changes in local volume fraction is not orderly. Last is the conclusions drawn from comparing the impact of changes to local and mean volume fraction changes.

The results in Section 3.2, for the investigated drag laws, for the most part are remarkably similar. They are predominately an exponential behavior, with Bogner et al. [4] behaving differently. This behavior, however, is most likely from the volume fraction being beyond the applicable range of the correlation. The other six correlations are also very close in magnitude, with Gidaspow [2] and Syamlal & O'Brien [1] being noticeably lower in magnitude. This isn't surprising, as those two drag laws predict a much less drastic change in drag for changes in average volume fraction, which can be seen in Figure 3.2.

The second conclusion is seen very clearly in Figure 4.3 – Figure 4.6, which is the local drag fluctuations are chaotic. Local drag fluctuations do not seem to have a dependence on the fluctuations in local volume fraction, and any dependence which might be present would have to involve other parameters. More so, the drag fluctuations seem to be evenly distributed around the (0,0) point of the graph. This suggests accounting for the fluctuations was no different than treating it as a homogeneous system without any fluctuations, which is of course to use the mean values. The drag laws investigated do just this to handle the drag of the system.

The third conclusion is from the comparison of the changes in drag from local and mean volume fraction changes. For very small mean and local volume fraction changes, the

change in drag was potentially comparable. It is only potentially the case as, due to the randomness of the local drag fluctuations, they may be very close or may be significantly different. However, very quickly the mean volume fraction changes produce a more significant impact on the mean drag of the system than the local volume fraction fluctuations do on the local drag. This means the response of the whole system to changes is much more impactful than local responses to changes. Ultimately this works to support aforementioned conclusion, which is a system can be adequately modeled by looking at the mean characteristics of the system without worrying about local fluctuations in the system.

REFERENCES

- [1] M. Syamlal and T. O'Brien, "A generalized drag correlation for multiparticle systems.," 1987.
- [2] D. Gidaspow, "Multiphase Flow and Fluidization," *Academic Press*, 1994.
- [3] R. Beetstra, M. A. van der Hoef and J. A. M. Kuipers, "Drag force of intermediate Reynolds number flows past mono- and bidisperse arrays of spheres," *AIChE J.*, vol. 53, pp. 489-501, 2007.
- [4] S. Bogner, S. Mohanty and S. Rude, "Drag correlation for dilute and moderately dense fluid-particle systems using the lattice Boltzmann method," *Int. J. Multiphase Flow*, vol. 68, pp. 71-79, 2015.
- [5] S. Tenneti, R. Garg and S. Subramaniam, "Drag law for monodisperse gas-solid systems using particle-resolved direct numerical simulation of flow past fixed assemblies of spheres," *Int. J. Multiphase Flow*, vol. 37, no. 9, pp. 1072-1092, 2011.
- [6] Y. Tang, E. A. J. F. Peters, J. A. M. Kuipers, S. H. L. Kriebitzsch and M. A. van der Hoef, "A new drag correlation from fully resolved simulations of flow past monodisperse static arrays of spheres," *AIChE J.*, vol. 61, no. 2, 2014.
- [7] A. A. Zaidi, T. Tsuji and T. Tanaka, "A new relation of drag force for high Stokes number monodisperse spheres by direct numerical simulation," *Adv. Powder Technol.*, vol. 25, no. 6, pp. 1860-1871, 2014.
- [8] M. Mehrabadi, Analysis of gas-solid flow using particle-resolved direct numerical simulation: flow physics and modeling, PhD Thesis, Iowa State University, 2016.
- [9] J. Lundberg and B. M. Halvorsen, "A review of some existing drag models describing the interaction between phases in a bubbling fluidized bed," in *49th Scand. Conf. Simulation and Modeling*, 2008.
- [10] G. Akiki, T. Jackson and S. Balachandar, "Force variation within arrays of monodisperse spherical particles," *Physical Review Fluids*, vol. 1, no. 4, August 2016.
- [11] R. Garg, "Modeling and simulation of two-phase flows," 2009.
- [12] S. Tenneti, "Momentum, energy and scalar transport in polydisperse gas-solid flows using particle-resolved direct numerical simulations," 2013.

APPENDIX. MATLAB CODE

This appendix contains the MATLAB code used to generate the graphs presented in Chapter 3.

```

clc
close all

%Parameters for simulation
phiList = [0.1 0.201 0.3 0.4]; %All the values of phi change to try
ReList = [0.01 1 5 10 20 30 40 50 100]; %List of Rem to try
D = 1; %Particle diameter
MU = 0.0012; %Particle viscosity
RHO = 1; %Particle density
m=2; %For forming subplots
n=2; %For forming subplots

%Symbolic variables for each drag law
syms TGS(phi,Re,d,mu,rho) %Tenneti et al
syms BVK(phi,Re,d,mu,rho) %Beetstra et al
syms ZA1(phi,Re,d,mu,rho) %Zaidi et al - Re <= 200
syms ZA2(phi,Re,d,mu,rho) %Zaidi et al - Re > 200
syms ZAI(phi,Re,d,mu,rho) %Zaidi et al - Complete
syms BOG(phi,Re,d,mu,rho) %Bogner et al
syms TAG(phi,Re,d,mu,rho) %Tang et al
syms WY(phi,Re,d,mu,rho) %Wen and Yu
syms ERG(phi,Re,d,mu,rho) %Ergun Equation for use in Gidaspow
syms GDS(phi,Re,d,mu,rho); %Gidaspow et al
syms SOB(phi,Re,d,mu,rho) %Syamlal & O'Brien

%Other symbolic variables used
syms SOBCd(phi,Re) %Drag Coefficient for Syamlal & O'Brien
syms vr(phi,Re) %Velocity correlation factor for Syamlal & O'Brien
syms Fst(phi,Re,d,mu,rho); %Stokes drag force
syms NumDen(phi,d); %Number Density
syms uf(phi,Re,d,mu,rho); %Fluid velocity
syms dPhi; %Change in volume fraction

%List of Figure Created
VerFig = figure('Name','Drag Law Verification','NumberTitle','off');
TGSFig = figure('Name','Tenneti et al','NumberTitle','off');
BVKFig = figure('Name','Beetstra et al','NumberTitle','off');
ZAIFig = figure('Name','Zaidi et al','NumberTitle','off');
BOGFig = figure('Name','Bogner et al','NumberTitle','off');
TAGFig = figure('Name','Tang et al','NumberTitle','off');
GDSFig = figure('Name','Gidaspow et al','NumberTitle','off');
SOBFig = figure('Name','Syamlal & OBrien','NumberTitle','off');

```

```
%Assign equations to symbolic variables for use in drag laws
```

```
uf(phi,Re,d,mu,rho) = (Re*mu)/(rho*d*(1-phi));
NumDen(phi,d) = (6*phi)/(pi*d^3);
Fst(phi,Re,d,mu,rho) = 3*pi*mu*d*(1-phi)*uf(phi,Re,d,mu,rho);
vr(phi,Re) = piecewise(phi>=0.15, 0.5*((1-phi)^4.14-
0.06*Re)+0.5*sqrt((0.06*Re)^2+0.12*Re*(2*0.8*(1-phi)^1.28-(1-phi)^4.14)+((1-phi)^4.14)^2),
phi<0.15, 0.5*((1-phi)^4.14-0.06*Re)+0.5*sqrt((0.06*Re)^2+0.12*Re*(2*(1-phi)^2.65-(1-
phi)^4.14)+((1-phi)^4.14)^2));
SOBCd(phi,Re) = (0.63+4.8/sqrt(Re./vr(phi,Re)))^2;
```

```
%Assign equations to symbolic variables for each drag law, corresponding to
%the form shown in Table 1.1
```

```
TGS(phi,Re,d,mu,rho) = ((1+0.15*Re^0.687)/(1-phi)^3 + (5.81*phi)/(1-phi)^3 +
0.48*(phi^(1/3)/(1-phi)^4) + phi^3*Re*(0.95+ (0.61*phi^3)/(1-
phi)^2)).*NumDen(phi,d).*Fst(phi,Re,d,mu,rho);
BVK(phi,Re,d,mu,rho) = ((10*phi)/(1-phi)^3 + (1-phi)*(1+1.5*sqrt(phi)) + ((0.413*Re)/(24*(1-
phi)^3))*((1-phi)^(-1)+3*phi*(1-phi)+8.4*Re^(-0.343))/(1+10^(3*phi)*Re^(-
(1+4*phi)/2))).*NumDen(phi,d).*Fst(phi,Re,d,mu,rho);
ZAI(phi,Re,d,mu,rho) = ((10*phi)/(1-phi)^3 + (1-phi)*(1+1.5*sqrt(phi)) + (0.034/(1-
phi)^3.7)*Re).*NumDen(phi,d).*Fst(phi,Re,d,mu,rho);
ZA2(phi,Re,d,mu,rho) = ((10.9*phi^0.4)/(1-phi)^2.7 + (0.024/(1-
phi)^3.86)*Re).*NumDen(phi,d).*Fst(phi,Re,d,mu,rho);
ZAI(phi,Re,d,mu,rho) = piecewise(Re<=200, ZAI(phi,Re,d,mu,rho), Re>200,
ZA2(phi,Re,d,mu,rho));
BOG(phi,Re,d,mu,rho) = ((1-phi)^(-5.726)*(1.751+0.151*Re^0.687-0.445*(1+Re)^(1.04*phi)-
0.16*(1+Re)^(0.0003*phi))).*NumDen(phi,d).*Fst(phi,Re,d,mu,rho);
TAG(phi,Re,d,mu,rho) = ((10*phi)/(1-phi)^3 + (1-phi)*(1+1.5*sqrt(phi)) + (0.11*phi*(1+phi) -
0.00456/(1-phi)^4 + (0.169*(1-phi) + 0.0644/(1-phi)^4)*Re^(-0.343))*(Re/(1-
phi))).*NumDen(phi,d).*Fst(phi,Re,d,mu,rho);
WY(phi,Re,d,mu,rho) = ((3*rho*(1-phi)*phi)/(4*d))*((24/Re)*(1+0.15*Re^(0.687)))*(1-phi)^(-
2.65).*uf(phi,Re,d,mu,rho).*uf(phi,Re,d,mu,rho);
ERG(phi,Re,d,mu,rho) = (150*((mu*phi^2)/((1-phi)*d^2)) +
1.75*(rho*phi.*uf(phi,Re,d,mu,rho)/d)).*uf(phi,Re,d,mu,rho);
GDS(phi,Re,d,mu,rho) = piecewise(phi<0.2, WY(phi,Re,d,mu,rho), phi>=0.2,
ERG(phi,Re,d,mu,rho));
SOB(phi,Re,d,mu,rho) = ((3*(1-
phi)*phi*rho)/(4*d.*vr(phi,Re).^2)).*SOBCd(phi,Re).*uf(phi,Re,d,mu,rho).^2;
```

```
%Plot for verification against results from Lundberg & Halvorsen
```

```
figure(VerFig)
```

```
v1 = fplot(TGS(phi,1.4,0.000154,0.000017894,1.225),[0 0.7], 'b-');
hold on
v2 = fplot(BVK(phi,1.4,0.000154,0.000017894,1.225),[0 0.7], 'r-');
v3 = fplot(ZAI(phi,1.4,0.000154,0.000017894,1.225),[0 0.7], 'k-');
v4 = fplot(BOG(phi,1.4,0.000154,0.000017894,1.225),[0 0.7], 'b--');
v5 = fplot(TAG(phi,1.4,0.000154,0.000017894,1.225),[0 0.7], 'r--');
v6 = fplot(GDS(phi,1.4,0.000154,0.000017894,1.225),[0 0.7], 'k--');
v7 = fplot(SOB(phi,1.4,0.000154,0.000017894,1.225),[0 0.7], 'cd');
hold off
legend([v1 v2 v3 v4 v5 v6
v7],{'Tenneti', 'Beetstra', 'Zaidi', 'Bogner', 'Tang', 'Gidaspow', 'Syamla
OBrien'}, 'Location', 'northwest');
ylabel('C_{F_{d}}')
```

```

xlabel('\phi')
title('Drag Law Validation')
ylim([0 180000])
xticks([0:0.1:0.7])
yticks([0:20000:180000])
set(gca,'xMinorTick','on','yMinorTick','on')

% dF/F(phi_0) vs. dPhi for Varying Re for each drag law
% Done using fplot, which plots expressions over a given range for a
% variable, which in this case is dPhi

% Tenneti et al
figure(TGSFig)
for i=1:length(phiList)
    subplot(m,n,i);
    for j=1:length(ReList)
        fplot((TGS(dPhi+phiList(i),ReList(j),D,MU,RHO)-
TGS(phiList(i),ReList(j),D,MU,RHO))./TGS(phiList(i),ReList(j),D,MU,RHO),[-phiList(i) 0.35])
        hold on
    end
    hold off
    title(['\phi_{0}=' num2str(phiList(i))])
    xlabel('\Delta\phi')
    ylabel('\Delta F/F(\phi_{0})')
    legend(strcat('Re=',num2str(ReList)), 'Location', 'northwest')
end

% Beetsra et al
figure(BVKFig)
for i=1:length(phiList)
    subplot(m,n,i);
    for j=1:length(ReList)
        fplot((BVK(dPhi+phiList(i),ReList(j),D,MU,RHO)-
BVK(phiList(i),ReList(j),D,MU,RHO))./BVK(phiList(i),ReList(j),D,MU,RHO),[-phiList(i) 0.35])
        hold on
    end
    hold off
    title(['\phi_{0}=' num2str(phiList(i))])
    xlabel('\Delta\phi')
    ylabel('\Delta F/F(\phi_{0})')
    legend(strcat('Re=',num2str(ReList)), 'Location', 'northwest')
end

% Zaidi et al
figure(ZAIFig)
for i=1:length(phiList)
    subplot(m,n,i);
    for j=1:length(ReList)
        fplot((ZAI(dPhi+phiList(i),ReList(j),D,MU,RHO)-
ZAI(phiList(i),ReList(j),D,MU,RHO))./ZAI(phiList(i),ReList(j),D,MU,RHO),[-phiList(i) 0.35])
        hold on
    end
    hold off
    title(['\phi_{0}=' num2str(phiList(i))])

```

```

xlabel('\Delta\phi')
ylabel('\Delta F/F(\phi_{0})')
legend(strcat('Re=', num2str(ReList)), 'Location', 'northwest')
end

%Bogner et al
figure(BOGFig)
for i=1:length(phiList)
    subplot(m,n,i);
    for j=1:length(ReList)
        dF=[];
        dPhiList=[];
        for dPhi=-phiList(i):0.05:0.35
            dF = [dF double((BOG(dPhi+phiList(i), ReList(j), D, MU, RHO) -
BOG(phiList(i), ReList(j), D, MU, RHO))/BOG(phiList(i), ReList(j), D, MU, RHO))];
            dPhiList = [dPhiList dPhi];
        end
        plot(dPhiList, dF)
        hold on
    end
    hold off
    title(['\phi_{0}= ' num2str(phiList(i))])
    xlabel('\Delta\phi')
    ylabel('\Delta F/F(\phi_{0})')
    legend(strcat('Re=', num2str(ReList)), 'Location', 'northwest')
end

%Tang et al
figure(TAGFig)
for i=1:length(phiList)
    subplot(m,n,i);
    for j=1:length(ReList)
        fplot((TAG(dPhi+phiList(i), ReList(j), D, MU, RHO) -
TAG(phiList(i), ReList(j), D, MU, RHO))./TAG(phiList(i), ReList(j), D, MU, RHO), [-phiList(i) 0.35])
        hold on
    end
    hold off
    title(['\phi_{0}= ' num2str(phiList(i))])
    xlabel('\Delta\phi')
    ylabel('\Delta F/F(\phi_{0})')
    legend(strcat('Re=', num2str(ReList)), 'Location', 'northwest')
end

%Gidaspow et al
figure(GDSFig)
for i=1:length(phiList)
    subplot(m,n,i);
    for j=1:length(ReList)
        fplot((GDS(dPhi+phiList(i), ReList(j), D, MU, RHO) -
GDS(phiList(i), ReList(j), D, MU, RHO))./GDS(phiList(i), ReList(j), D, MU, RHO), [-phiList(i) 0.35])
        hold on
    end
    hold off
    title(['\phi_{0}= ' num2str(phiList(i))])

```

```

xlabel('\Delta\phi')
ylabel('\Delta F/F(\phi_{0})')
legend(strcat('Re=',num2str(ReList)), 'Location', 'northwest')
end
%}

%Syamlal & O'Brien
figure(SOBFig)
for i=1:length(phiList)
    subplot(m,n,i);
    for j=1:length(ReList)
        dF=[];
        dPhiList=[];
        for dPhi=-phiList(i):0.05:0.35
            dF = [dF double((SOB(dPhi+phiList(i),ReList(j),D,MU,RHO)-
SOB(phiList(i),ReList(j),D,MU,RHO))/SOB(phiList(i),ReList(j),D,MU,RHO))];
            dPhiList = [dPhiList dPhi];
        end
        plot(dPhiList,dF)
        hold on
    end
    hold off
    title(['\phi_{0}=' num2str(phiList(i))])
    xlabel('\Delta\phi')
    ylabel('\Delta F/F(\phi_{0})')
    legend(strcat('Re=',num2str(ReList)), 'Location', 'northwest')
end

```